A Novel Method for Measuring the MTF of CT Scanners: A Phantom Study

Hamidreza Khodajou-Chokami, *Member, IEEE*, Seyed Abolfazl Hosseini, Mohammad Reza Ay, *Member, IEEE,* Ali Safarzadehamiri, Pardis Ghafarian, Habib Zaidi, *Member, IEEE*.

The modulation transfer function (MTF) is well known as a crucial parameter in quality assurance of computed tomography (CT) scanners, which provides detailed information of both contrast and resolution of CT images. Different methods have been introduced and developed to calculate the MTF of CT scanners. However, a robust methodology which accurately estimates the MTF of CT scanners under the use of every range of object electron density and tube current-time product (mAs) has not been reported so far. To this aim, a new wavelet-based circular edge method for MTF measurement has been presented in this work. Owning to the edge spread function (ESF) susceptibility to noise, the approach was based on the assumption that the ESF can be decomposed into approximate and detailed information containing different noise levels. To evaluate the performance of our method, an in-house fabricated phantom containing various disk objects covering a range of electron densities from low to high values was scanned by a volumetric 64-slice clinical CT scanner under a range of low tube current from 50 to 100 mAs where image noise levels are higher than those of normal-dose scan protocols. Measurements have shown that our proposed method yielded an accurate estimation of MTF for high-density as well as low-density disk objects and it is valid and stable over the variations of noise levels.

Keywords—*Modulation transfer function, Computed Tomography, Wavelet transform, noise, electron density, signal decomposition.*

This work was supported in part by Sharif University of Technology under a Graduate Research Program Grant.

H. Khodajou-Chokami is with the Group of Medical Radiation Engineering, Department of Energy Engineering, Sharif University of Technology, Tehran, Iran (e-mail: hamidreza.khodajou@gmail.com).

S. A Hosseini is with the Group of Medical Radiation Engineering, Department of Energy Engineering, Sharif University of Technology, Tehran, Iran (e-mail: sahosseini@sharif.edu).

M. R. Ay is with the Department of Medical Physics and Biomedical Engineering, Tehran University of Medical Sciences, Tehran, Iran (e-mail: mohammadreza_ay@tums.ac.ir).

A. Safarzadehamiri is with the Group of Radiation Application Engineering, Department of Energy Engineering, Sharif University of Technology, Tehran, Iran (e-mail: ali.amiri1371s76@gmail.com).

P. Ghafarian is with the Group of Chronic Respiratory Diseases Research Center, National Research Institute of Tuberculosis and Lung Diseases (NRITLD), Shahid Beheshti University of Medical Sciences. Tehran, Iran (e-mail: pardis.ghafarian@sbmu.ac.ir).

H. Zaidi is with the Department of Medical Physics and Biomedical Engineering, Tehran University of Medical Sciences, Tehran, Iran (habib.zaidi@hcuge.ch).

I. Introduction

The modulation transfer function (MTF) is one of the most important parameters in performance evaluation and quality assurance of computed tomography (CT) scanners [1-5]. A number of techniques were proposed for the measurement of the MTF, involving the use of either commercial or in-house fabricated phantoms [5-8]. Moreover, one of the recent advances in CT imaging has been the development of iterative reconstruction algorithms, which improves the noise properties, contrast and enables to handle other nonlinear factors, such as metallic artifacts [8, 9]. Therefore, deriving a robust method for measurement of the MTF using an edge method which could yield promising and accurate results for any imaging protocol is desirable.

Various edge methods for MTF estimation have been reported by other groups. Judy *et al* [6] estimated the line spread function (LSF) and MTF of the EMI CT brain scanner using a step function obtained by placing a block of Perspex in the water bath. Boone *et al* [7] measured the MTF by calculating the LSF using an in-house built phantom consisting of a thin aluminum foil. Friedman *et al* [8] and Richard *et al* [10] measured the MTF of a clinical CT scanner using the circular edge of a disk-shaped object which was part of the American College of Radiology (ACR) phantom. Because the LSF obtained from the first derivative of the edge spread function (ESF), the proposed techniques are strongly affected by noise and contrast of background material compared to that of the disk. Thus, it is essential to suppress these factors on the ESF. To reduce the impact of image noise on the ESF, Friedman *et al* [8] averaged phantom slices along the z-direction on a voxel-by-voxel basis to create a single low-noise axial image while Richard *et al* [10] employed an averaged ESF obtained by consecutive CT slices. By applying these approaches, not only a moderate amount of noise still remains in the process of MTF estimation but also a slight misalignment of the phantom edge between slices can decrease the accuracy of the MTF measurement. Subsequent work by Wilson and colleagues [11] has shown that the use of a Savitzky–Golay smoothing filter [12] reduces the impact of noise on the ESF. However, they were unable to provide a reliable MTF from a low-density rod because its image contrast and noise were too low and too high, respectively. Nonetheless, a reliable method for the accurate estimation of the MTF of CT scanners against the variability of noise levels and electron densities of materials has not been reported.

978-1-5386-8428-3/19/$31.00 ©2019 IEEE

This work introduces a novel wavelet-based circular edge technique for assessing the spatial resolution of CT scanners, which is resilient to noise. The validity and reliability of our method have been evaluated. The method uses an in-house fabricated phantom consisting of a number of rods with electron densities covering a range of HU values from the lower to higher HU compared to HU of the background. The effects of disk contrast and various acquisition parameters on the MTF measurement have also been investigated.

II. Materials and Methods

A. CT Scanner Specification and Experimental Setup

The volumetric 64-slice GE LightSpeed™ VCT scanner (GE Healthcare Technologies, Waukesha, WI) was used for data acquisition. The detector array consists of 58,368 individual elements configured in 64 rows of 0.0625 cm thickness on the z-axis and 0.055 cm on the x-axis at isocenter, each containing of 888 active patient elements and 24 reference elements with $Y_{1.34}Gd_{0.60}Eu_{0.06}O_3$ scintillator. The scanner uses Performix Pro Anode Grounded Metal-Ceramic Tube Unit with two focal spots. The small and large focal spot sizes are 0.09 cm (width) × 0.07 cm (length) and 0.12 cm (width) × 0.12 cm (length), respectively. The tube anode target is made of Tungsten and the angle of the target is 7°. The x-ray beam is collimated to a fan-angle of 56°. The tube's minimum inherent and additional filtrations are 3.25 mm Al and 0.1 mm Cu at 140 kV, respectively. The maximum scan field-of-view is 50 cm and the distances of the source to isocenter and source to the detector are 54 cm and 95 cm, respectively. The phantom (described in section 2.B) was scanned the acquisition parameters summarized in Table I. The reconstruction of axial images was performed using the filtered backprojection (FBP) algorithm with a standard reconstruction kernel.

TABLE I. Details of the acquisition parameters used to scan the phantoms.

Scan type	Axial
Tube voltage (kVp)	120
Tube current-time product (mAs)	50, 75, 100 and 125
Scan field-of-view (cm)	30
Slice thickness (cm)	0.25
Pixel size (mm^2)	0.586 × 0.586

B. Phantoms

A water-filled cylindrical phantom containing two modules, shown in Fig. 1 was used to measure the MTF. The multi-disk module (Fig. 1(a)) was made of four 4 cm diameter rods containing Teflon (a bone tissue equivalent material), low-density polyethylene (LDPE), acrylic and solid water (background material) with nominal CT Hounsfield unit (HU) values of 990, -90, 120 and 0, respectively.

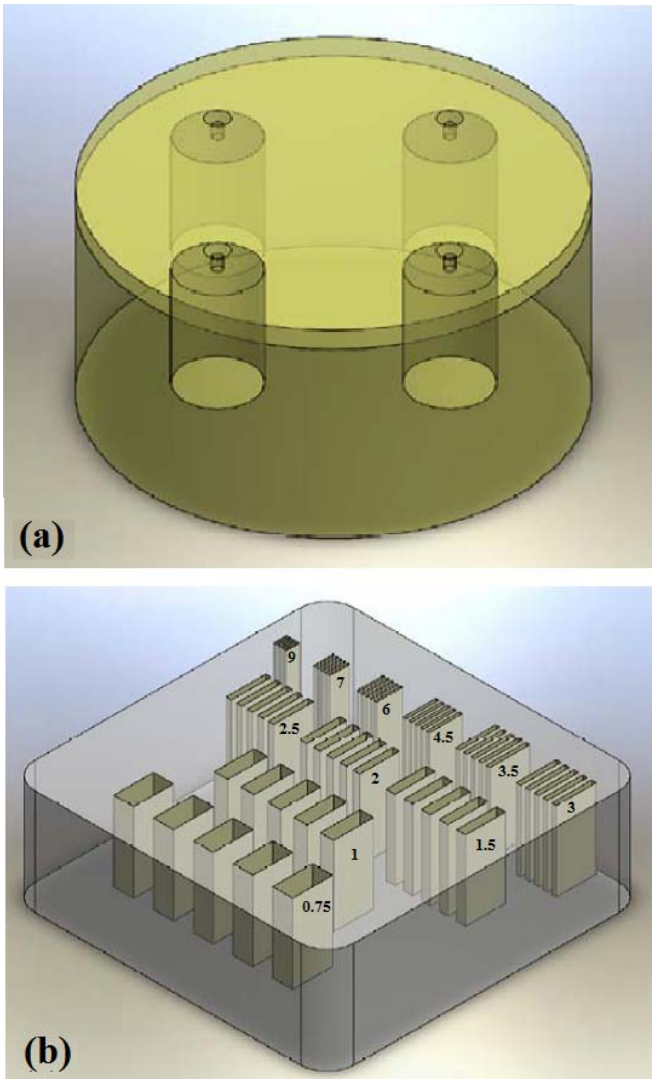

Fig. 1. A representation of our in-house fabricated phantom containing (a) multi-disk module (b) bar-pattern module used to calculate the MTF of the CT scanner.

The bar-pattern module, displayed in Fig. 1(b), was made of Plexiglas including 11 groups containing 5 slits with spatial frequencies of 0.75–9 lp/cm. Fig. 2 shows representative axial slices of our in-house fabricated phantom acquired using GE's recommended standard scan protocol [13] for evaluation of our purposed methodology (described in the section 2.C) for the estimation of the spatial resolution.

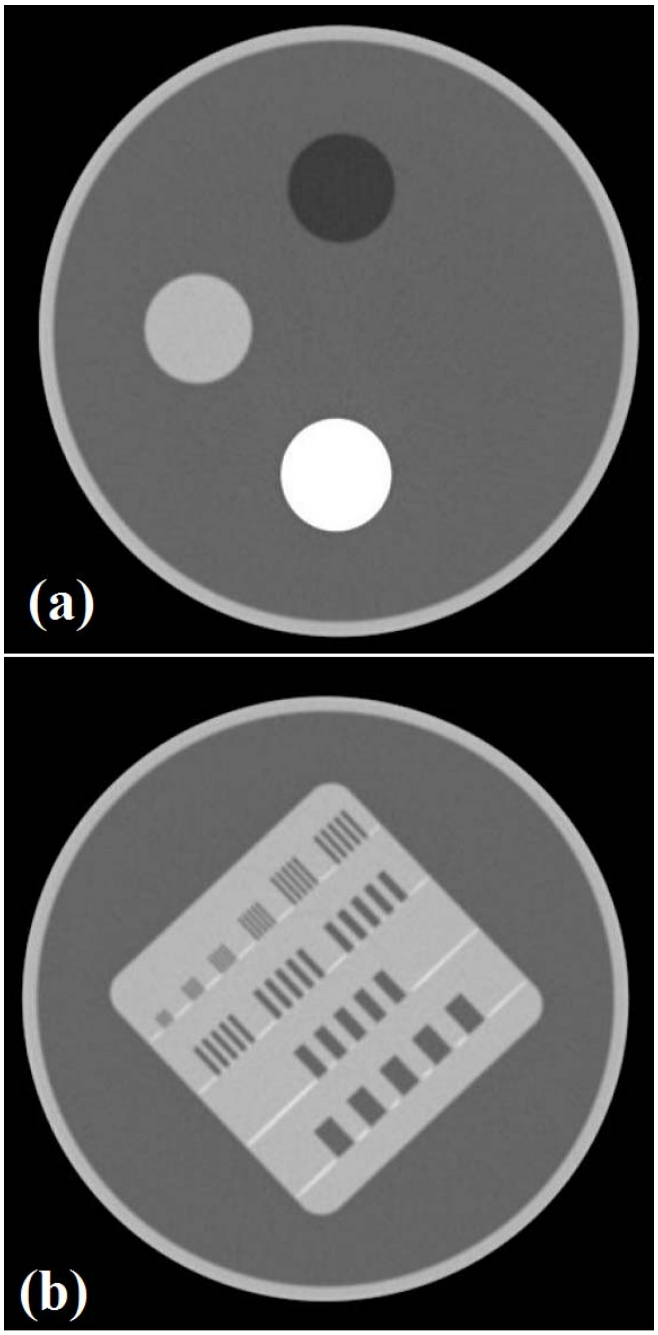

Fig. 2. Representative axial slices of our in-house fabricated phantom acquired using GE's recommended standard scan protocol for evaluation of the spatial resolution: (a) multi-disk module, and (b) bar-pattern module. The spatial frequencies of the patterns are in the range 0.75, 1, 1.5, 2, 2.5, 3, 3.5, 4.5, 6, 7 and 9 lp/cm from the largest to the smallest slits. The experimental axial image indicated that the limiting spatial resolution is between 6 and 7 lp/cm.

C. Method Measurement of the MTF

A new approach has been devised for accurate measurement of the MTF of CT scanners which remains practical under different noise levels and for various materials' electron densities. The foundation of this method lays on the principle of the edge method [14]. First, all pixel values of axial images were normalized using the following equation:

$$I_N(i,j) = \frac{HU(i,j) - \overline{HU_b}}{\overline{HU_O} - \overline{HU_b}} \quad (1)$$

where $HU(i,j)$ indicates HU value of the pixel at (i,j) location and $\overline{HU_O}$ and $\overline{HU_b}$ are average HU values of each rod and background, respectively. Second, every region of interest (ROI) was defined to correspond to one of the user selected rods. Then, the center coordinates and the radius of any rod image were identified using Otsu's thresholding method [15]. The oversampled ESF was calculated by rebinning as a function of distance from the center of the rod. That is, it is achieved by averaging the pixel values within each isocenter half donut shaped contours. We applied a 3-level wavelet decomposition of oversampled ESF to eliminate the noise as depicted in Fig. 3. The principle of the signal decomposition process was adapted from Mallat's algorithm [16]. In Fig. 3, H [n] is a high pass filter and L[n] is a low pass filter, whereas cj[n] and dj[n] denote approximation coefficients and detail coefficients, respectively. At each decomposition level, the filters yield signals which span only the half band of the frequency and the frequency resolution is doubled. According to Nyquist's theorem, down-sampling can be performed by a factor of 2 at the output of each filter. The important point to note is that by traveling towards higher decomposition levels, the noise will be eliminated as well. The LSF can be obtained by taking the first order central finite difference of the ESF as follows:

$$LSF(r) \approx \frac{ESF_{k+1} - ESF_{k-1}}{2(r_{k+1} - r_k)} \quad (2)$$

Thus, a radially symmetric MTF can be defined by taking the Fourier transformation of the LSF as follows:

$$MTF(r) = \frac{\int_0^{\infty} LSF(r).exp(-2\pi ifr)\,dr}{\int_0^{\infty} LSF(r)\,dr} \quad (3)$$

where the denominator satisfies the condition MTF (0) =1.

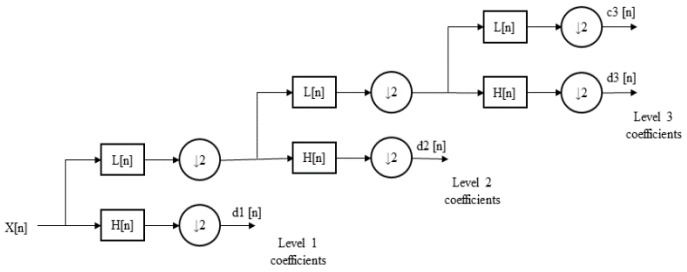

Fig. 3. Demonstration of a 3-level filter bank used for the decomposition of the oversampled ESF signal.

III. RESULTS AND DISCUSSIONS

Fig. 4 shows demonstrates the 3-level decomposition process of the ESF. Fig. 4 shows the rebinned ESF with one-tenth pixel size X[n] along with its approximation $c_3[n]$. Fig. 5 portrays a comparison of the MTF measurements obtained with and without applying the wavelet-based ESF decomposition. As shown in Fig. 5, the measured MTF

without applying the wavelet-based ESF decomposition fluctuates irregularly, especially at high spatial frequencies because of the noise remaining in the ESF signal. However, the MTF derived from the wavelet-based ESF decomposition indicates no fluctuations throughout the range of spatial frequencies. The performance evaluation of our purposed methodology is presented in figures 5-7.

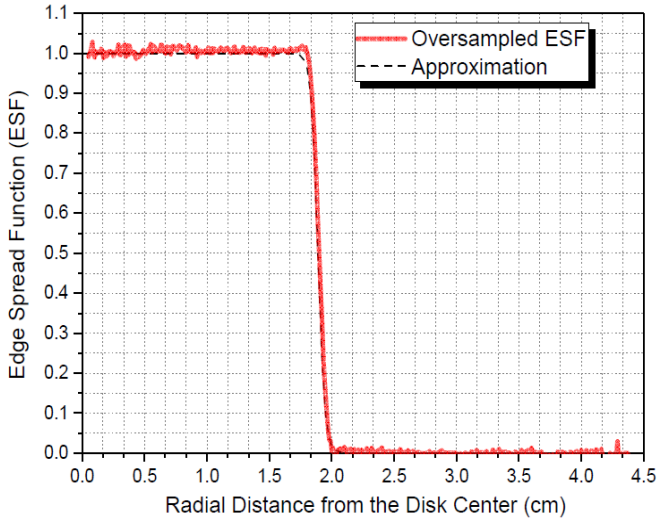

Fig. 4. Representation of the rebinned ESF with tenth pixel size x[n] and its approximation c3[n].

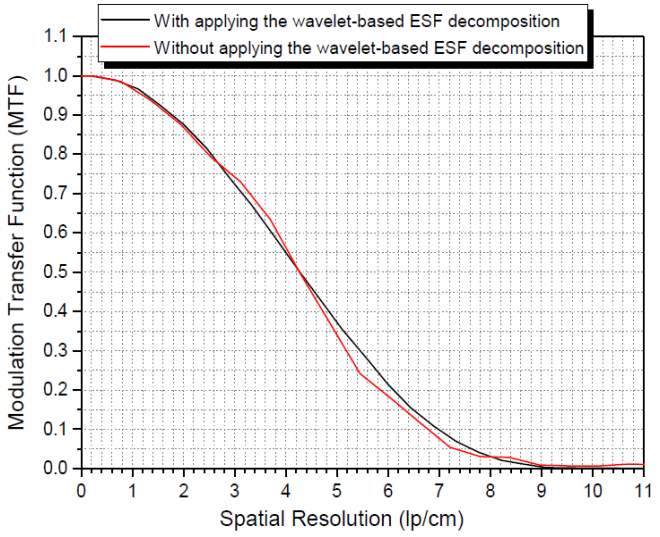

Fig. 5. Comparison of the MTF measurements obtained with and without applying the wavelet-based ESF decomposition.

Fig. 6 indicates the measured MTF as a function of spatial frequency across a wide range of tube fluences (50, 75, 100 and 125 mAs) covering different noise levelsdemonstrating that the MTFs has not affected by the tube current. These results have shown that our wavelet-based circular edge technique is robust for measuring the MTF of CT scanners, whereas the edge method was considerably affected by noise since it's derived from the ESF to calculate the LSF.

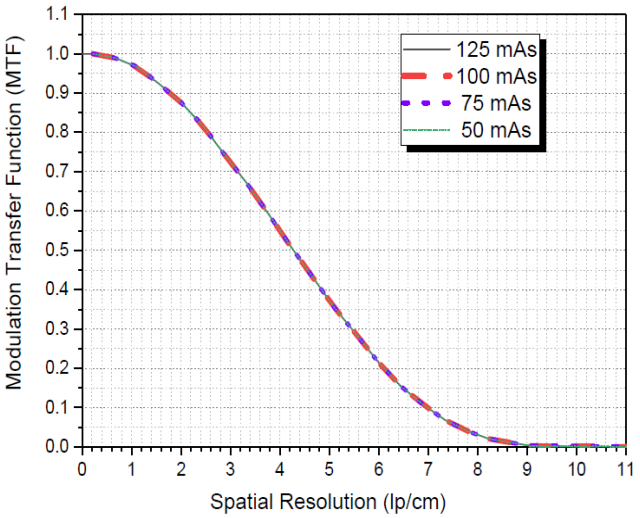

Fig. 6. The MTF as a function of spatial frequency measured by changing tube current-time product in the range of 50, 75, 100 and 125 mAs covering the typical level of low to normal scan dose.

Fig. 7 shows that the measured MTFs are slightly affected by different electron densities of disk objects. The 50% MTFs, which equates to 50% loss of contrast, were 4.273, 4.208 and 4.143 lp/cm for Teflon, acrylic and LDPE inserts with CT number values of 990, 120 and -90 HU, respectively. Although the measured 50% MTF value was degraded by low-contrast objects compared to a high-contrast object, the discrepancies between the maximum and minimum values of 50% MTF was about 0.13 and considered to be negligible from a practical viewpoint.

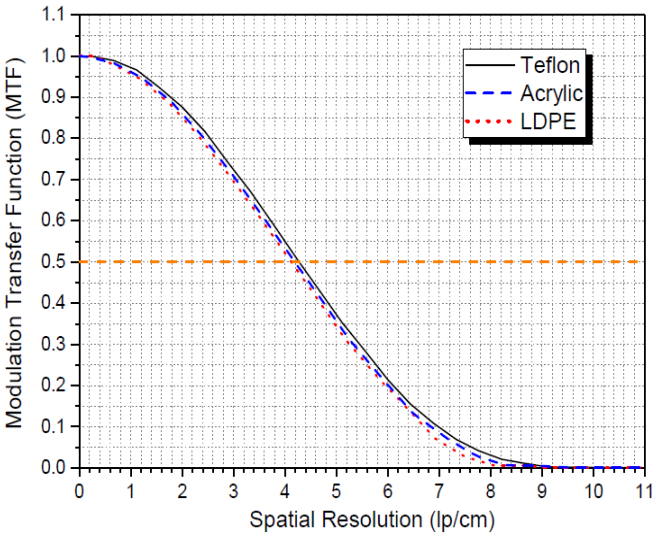

Fig. 7. The MTF as a function of spatial frequency measured by using different electron densities of disk objects including Teflon, LDPE and acrylic inserts.

The results shown in figures 4-7 derived by our method demonstrate that the limiting spatial resolution (10% MTF) of the volumetric 64-slice GE LightSpeed™ VCT scanner [17] is equal to 6.72 lp/cm whereas those obtained using the bar pattern indicated that it is between 6 and 7 lp/cm as shown in Fig. 2. All the above results are in agreement with

the manufacturer's expected values where the limiting spatial resolution was greater than or equal to 6.5 [13].

IV. Conclusions

We have presented a new methodology using the wavelet-based circular edge technique for measurement of the MTF of CT scanners. The accuracy of our proposed method was evaluated through comparison with the results of the bar pattern method as well as the GE manufacturer's published data [13] demonstrating a very good agreement. The results indicated the validity and stability of our proposed methodology for MTF measurement under the use of different ranges of noise levels and electron densities of materials. Therefore, it seems to be a suitable approach for radial MTF measurement for both low-contrast and high-contrast objects with a large amount of noise in CT images. It is presumably the concept of our purposed technique would be useful for other imaging systems, including mammography [18], single photon emission computed tomography, positron emission tomography systems [19].

References

[1] Nowik P, Bujila R, Poludniowski G, Fransson A. Quality control of CT systems by automated monitoring of key performance indicators: a two-year study. J Appl Clin Med Phys. 16:254–265, 2015.

[2] Mori I. Non-linear Nature of Recent CT Images and Image Quality Evaluation. Bull Sch Health Sci Tohoku Univ. 22:7–2, 2013.

[3] Nute JL, Rong J, Stevens DM, et al. Evaluation of over 100 scanner years of computed tomography daily quality control data. Med Phys. 40:051908–1, 2013.

[4] Husby E, et al. 100 days with scans of the same Catphan phantom on the same CT scanner. J Appl Clin Med Phys. 18:6: 224–231, 2017.

[5] American Association of Physicists in Medicine (AAPM). Phantoms for Performance Evaluation and Quality Assurance of CT Scanners. AAPM report No. 1, New York, Am. Inst. Phys., Diagnostic Radiology Committee Task Force on CT Scanner Phantoms; 1977.

[6] Judy P F The line spread function and modulation transfer function of a computed tomographic scanner, Med Phys. 3, 233–6, 1976.

[7] Boone JM. Determination of the presampled MTF in computed tomography. Med Phys. 28(3):356–60, 2001.

[8] Friedman SN, Fung GS, Siewerdsen JH, Tsui BM. A simple approach to measure computed tomography (CT) modulation transfer function (MTF) and noise-power spectrum (NPS) using the American College of Radiology (ACR) accreditation phantom. Med Phys. 40(5):051907, 2013.

[9] Takata T, et al, Object shape dependency of in-plane resolution for iterative reconstruction of computed tomography, *Phys Med*., 33: 146-151, 2017.

[10] Richard S, Husarik DB, Yadava G, Murphy SN, Samei E. Towards task-based assessment of CT performance: system an object MTF across different reconstruction algorithms. Med Phys. 39(7):4115–22, 2012.

[11] Wilson JM, Christianson OI, Richard S, Samei E. A methodology for image quality evaluation of advanced CT systems. Med Phys. 40(3):0319081–9, 2013.

[12] Schafer RW. What is a Savitzy–Golay filter? IEEE Signal Process Mag. 28:111–7, 2011.

[13] GE LightSpeed™ VCT scanner, Technical Reference Manual, 5340596-1EN Revision 5, 2011.

[14] Samei E, Flynn MJ. A method for measuring the presampled MTF of digital radiographic systems using an edge test device. Med Phys. 25(1):102–13, 1998.

[15] Otsu N. A threshold selection method from gray-level histograms. IEEE Trans Syst Man Cybern. 9(1):62–6, 1979.

[16] Mallat, S., A theory for multiresolution signal decomposition: the wavelet representation, IEEE Pattern Anal. and Machine Intell. 11: 674–693, 1989.

[17] H. Khodajou-Chokami, S. A. Hosseini, M. R. Ay, and H. Zaidi, "MCNPFBSM: Development of MCNP/MCNPX Source Model for Simulation of Multi-Slice Fan-Beam X-Ray CT Scanners," the 14th IEEE International Symposium on Medical Measurements and Applications, 2019.

[18] H. Khodajou-Chokami, M. Sohrabpour "Design of linear anti-scatter grid geometry with optimum performance for screen-film and digital mammography systems," Phys. Med. Biol. vol.60 p.5753, 2015.

[19] Rahmim, A. and Zaidi, H., PET versus SPECT: strengths, limitations and challenges. Nuclear medicine communications. 29: 193-207, 200